Nuclear Instruments and Methods in Physics Research A 767 (2014) 289–295

Contents lists available at ScienceDirect

Nuclear Instruments and Methods in Physics Research A

journal homepage: www.elsevier.com/locate/nima

Development of GAGG depth-of-interaction (DOI) block detectors based on pulse shape analysis

Seiichi Yamamoto [a,*], Takahiro Kobayashi [a,b], Jung Yeol Yeom [c], Yuki Morishita [a], Hiroki Sato [d], Takanori Endo [d], Yoshiyuki Usuki [d], Kei Kamada [e], Akira Yoshikawa [e,f]

[a] Nagoya University Graduate School of Medicine, Nagoya, Japan
[b] Department of Radiology, Daiyukai General Hospital, Ichinomiya, Japan
[c] Kumoh National institute of Technology, Gumi, South Korea
[d] Furukawa Corporation, Ichihara, Japan
[e] New Industry Creation Hatchery Center (NICHe), Tohoku University, Sendai, Japan
[f] Institute for Materials Research (IMR), Tohoku University, Tohoku, Japan

ARTICLE INFO

Article history:
Received 23 June 2014
Received in revised form
5 August 2014
Accepted 3 September 2014
Available online 10 September 2014

Keywords:
GAGG
Decay time
Pulse shape
DOI detector

ABSTRACT

A depth-of-interaction (DOI) detector is required for developing a high resolution and high sensitivity PET system. Ce-doped $Gd_3Al_2Ga_3O_{12}$ (GAGG fast: GAGG-F) is a promising scintillator for PET applications with high light output, no natural radioisotope and suitable light emission wavelength for semiconductor based photodetectors. However, no DOI detector based on pulse shape analysis with GAGG-F has been developed to date, due to the lack of appropriate scintillators of pairing. Recently a new variation of this scintillator with different Al/Ga ratios—Ce-doped $Gd_3Al_{2.6}Ga_{2.4}O_{12}$ (GAGG slow: GAGG-S), which has slower decay time was developed. The combination of GAGG-F and GAGG-S may allow us to realize high resolution DOI detectors based on pulse shape analysis. We developed and tested two GAGG phoswich DOI block detectors comprised of pixelated GAGG-F and GAGG-S scintillation crystals. One phoswich block detector comprised of $2 \times 2 \times 5$ mm pixel that were assembled into a 5×5 matrix. The DOI block was optically coupled to a silicon photomultiplier (Si-PM) array (Hamamatsu MPPC S11064-050P) with a 2-mm thick light guide. The other phoswich block detector comprised of $0.5 \times 0.5 \times 5$ mm (GAGG-F) and $0.5 \times 0.5 \times 6$ mm^3 (GAGG-S) pixels that were assembled into a 20×20 matrix. The DOI block was also optically coupled to the same Si-PM array with a 2-mm thick light guide. In the block detector of 2-mm crystal pixels (5×5 matrix), the 2-dimensional histogram revealed excellent separation with an average energy resolution of 14.1% for 662-keV gamma photons. The pulse shape spectrum displayed good separation with a peak-to-valley ratio of 8.7. In the block detector that used 0.5-mm crystal pixels (20×20 matrix), the 2-dimensional histogram also showed good separation with energy resolution of 27.5% for the 662-keV gamma photons. The pulse shape spectrum displayed good separation with a peak-to-valley ratio of 6.5. These results indicate that phoswich DOI detectors with the two types of GAGGs are promising for developing a high resolution PET system.

1. Introduction

Ce-doped $Gd_3Al_2Ga_3O_{12}$ (GAGG fast: GAGG-F) has been reported to be a promising scintillator for PET applications for its high light output [1]. In addition to high light output, GAGG-F has no natural radioisotope, and suitable light emission wavelength for semiconductor based photodetectors [1]. GAGG-F has reasonable timing resolution [2] and can resolve a small pixel block when coupled to a silicon photomultiplier (Si-PM) [3]. These properties of GAGG are advantageous to develop a high resolution PET system [4] such for applications as in-beam imaging of positron radionuclides [5,6] or micro dose testing [7] where the radioactivity of the subject is small and the accidental coincidence and beta-gamma coincidence from the natural radioactivity of Lu based scintillators [8,9] is a problem.

For developing a high resolution and high sensitivity PET system with a uniform spatial resolution across the entire field-of-view (FOV), a depth-of-interaction (DOI) detector is needed. The DOI detectors are more important for relatively lower density and atomic number scintillators such as GAGG because the penetration is more serious for these scitnillators. Numerous types of DOI detectors have been proposed for PET detectors [10–15], and some of them have been implemented into PET systems [16–22]. In some of these DOI detectors, pulse shape discrimination utilizing decay time differences of the scintillators were used to realize high

* Corresponding author.
E-mail address: s-yama@met.nagoya-u.ac.jp (S. Yamamoto).

http://dx.doi.org/10.1016/j.nima.2014.09.001
0168-9002/

resolution PET detectors. We have previously developed a silicon photomultiplier (Si-PM) based DOI PET system [17] and two integrated PET/MRI systems [18,19] using two types of LGSOs with different decay times. In addition, we developed DOI brain PET system using two types of GSO with different Ce concentrations [20]. Such phoswich configurations with the same types of scintillators are ideal for integration into a DOI detector because their density, emission light wavelength, refractive index, and light outputs are similar. Although LGSO and GSO are suitable scintillators for this purpose, no crystal counterpart that would allow one to realize a GAGG-based phoswich DOI detector was available. If a GAGG-based phoswich DOI detector is realized, it will be a promising candidate for high resolution Si-PM based PET system because the light wavelength of GAGG is suitable for silicon based photodetectors and good energy and positioning performance will be expected.

Recently, a new variation of the scintillator with different Al/Ga ratios—Ce-doped $Gd_3Al_{2.6}Ga_{2.4}O_{12}$ (GAGG-S), which has longer decay properties, was developed by Furukawa Corporation [23]. The combination of GAGG-F and GAGG-S with pulse shape discrimination can potentially realize high resolution DOI detectors. In this paper, we utilized GAGG-F and GAGG-S to realize a phoswich-based DOI detector for PET and report our first results with GAGG phoswich-based DOI detectors.

2. Materials and methods

2.1. Basic performance measurements of GAGG-F and GAGG-S

We measured the basic performances of GAGG-F and GAGG-S for their pulse shapes, energy spectra and timing resolution. The pulse shape was measured using single GAGGs ($5 \times 5 \times 5$ mm^3 and all polished surfaces) optically coupled to a 3-inch round photomultiplier tube (PMT: Hamamatsu R6233-100 HA), and the output signal was fed to a digital oscilloscope (Yokogawa DLM2052: 500 MHz, maximum sampling rate, 2.5 GS/s) with a 50-Ω resistor for termination. We plotted the data on a graph, conducted exponential fit and evaluated the decay time.

The energy spectra were also acquired using the same PMT, readout with a standard NIM module whose outputs are fed to a multi-channel analyzer (ADC Model 1125P, Clear-Pulse Co., Tokyo). A Cs-137 point source was used for both of the above measurements.

The timing resolution measurements for a pair of GAGG scintillators were conducted using Si-PM (Hamamatsu MPPC S12573, 3 mm × 3 mm input area) readout with high speed amplifiers (mini circuit, TB-408-3+) and a digital oscilloscope (Agilent Technology DSO-8104A: 1 GHz, 20 Gs/s). The details of this digital oscilloscope based timing resolution evaluation method are reported in [24]. A pair of GAGG pixels ($3 \times 3 \times 3$ mm^3) was optically coupled to individual Si-PMs and fed to the digital oscilloscope based timing evaluation system. Data processing as described in the paper was conducted offline using MATLAB. A Na-22 point source was used for these measurements.

2.2. Phoswich DOI block detectors

Two types of GAGG phoswich block detectors have been developed; one with $2 \times 2 \times 5$ mm^3 crystal pixels assembled into a 5×5 matrix (large pixel block), and the other with $0.5 \times 0.5 \times 5$ mm^3 (GAGG-F) and $0.5 \times 0.5 \times 6$ mm^3 (GAGG-S) pixels, which were assembled into a 20×20 matrix (small pixel block). The large pixel block was initially used to evaluate the feasibility of our proposed phoswich DOI detector and the small pixel block for testing the possibility of fabricating ultra-high resolution DOI block detectors.

(1) Large pixel block
In the large pixel block, two types of GAGGs (GAGG-F and GAGG-S) with $2 \times 2 \times 5$ mm^3 pixel were put together into a 5×5 matrix with a 0.1 mm thick $BaSO_4$ reflector and optically coupled to each other in the depth direction to form a DOI block, which was optically coupled to a Si-PM array (Hamamatsu MPPC S11064-050P) with a 2-mm thick light guide using silicone rubber (Sin-etsu Silicone, KE-420). Fig. 1 shows the large pixel block detector, where the upper layer is the GAGG-F array and the lower layer is the GAGG-S array. We set the upper layer with GAGG-F array because count rate performance may slightly be better with the configuration. A Cs-137 point source was used for the measurement.

(2) Small pixel block
In the small pixel block, two types of GAGGs (GAGG-F and GAGG-S) with $0.5 \times 0.5 \times 5$ mm^3 pixel (GAFF-F) and $0.5 \times 0.5 \times 6$ mm^3 pixel (GAFF-S) were assembled into a 20×20 matrix with a 0.1-mm thick $BaSO_4$ reflector and optically coupled to each other in the depth direction to form a DOI block, which was also optically coupled to an identical Si-PM array with a 2-mm thick light guide using the same silicone rubber. Fig. 2 shows the small pixel block detector in its final assembled form. The upper layer is the GAGG-F array, while the lower layer is the GAGG-S array.

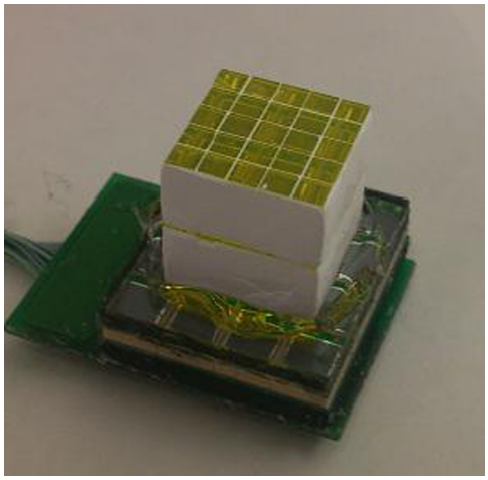

Fig. 1. Photograph of developed Si-PM-based GAGG phoswich large pixel block detector. The top surface of GAGG block was covered with white Teflon reflector when we measured the performance.

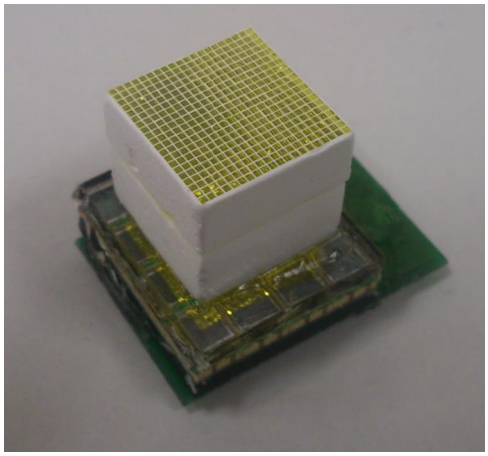

Fig. 2. Photograph of developed Si-PM-based GAGG phoswich small pixel block detector. The top surface of GAGG block was covered with white Teflon reflector when we measured the performance.

(3) Data processing and evaluation

The current signals from the sixteen Si-PM channels are transferred to a weighted summing board by 1.2-m-long, thin diameter coaxial cables, terminated by 25 Ω resistors, and converted to voltage signals. The voltage signals are individually amplified by voltage feedback high speed operational amplifiers (AD 8056, Analog Devices) and summed into rows and columns using summing amplifiers. These signals are weighted summed with position dependent linear gains for each row and column to produce weighted sum signals. We fed the weighed sum signals to 100-MHz analog to digital (A–D) converters of the data acquisition system, integrated them with two different integration times (230 and 470 ns), and calculated their positions using the Anger principle by full integration (470 ns) and pulse shape analysis by calculating the ratio of partial (230 ns) to full (470 ns) integrations in an FPGA. These integration times were experimentally determined to produce proper separations in the pulse shape spectra. The electronics used in this study are identical to our previously developed Si-PM PET system [17], but the integration times were longer because of the longer decay times of the GAGGs than LGSOs. We measured the 2-dimensional distribution, the pulse shape spectra, and the energy spectra for both the GAGG phoswich detectors with large and small pixel blocks.

3. Results

3.1. Basic performance measurement of single GAGG-F and GAGG-S

Fig. 3 shows the pulse shapes of GAGG-F and GAGG-S measured by the digital oscilloscope. Totally, 1024 events were averaged for the graphs. Their measured decay times were 110 ± 2 and 183 ± 5 ns for GAGG-F and GAGG-S, respectively.

The energy spectra of GAGG-F and GAGG-S acquired by the MCA are illustrated in Fig. 4. From the figure, it is clear that the photo-peak channels are largely overlapping, indicating almost identical light output. The energy resolutions for GAGG-F and GAGG-S were$7.5 \pm 0.2\%$ and $6.3 \pm 0.3\%$ FWHM, respectively.

The optimal timing resolutions for GAGG-F and GAGG-S obtained using the digital oscilloscope based timing resolution evaluation system are 419 ± 12 ps and 1259 ± 50 ps for GAGG fast and slow, respectively. The timing resolution of the GAGG-F pixel pair was ~1/3 of that of GAGG-S.

Table 1 summarizes our measured results in addition to the major properties of GAGG-F and GAGG-S. Except for the decay time and timing resolution, most of their properties are similar which is an advantage for phoswich-based DOI detectors.

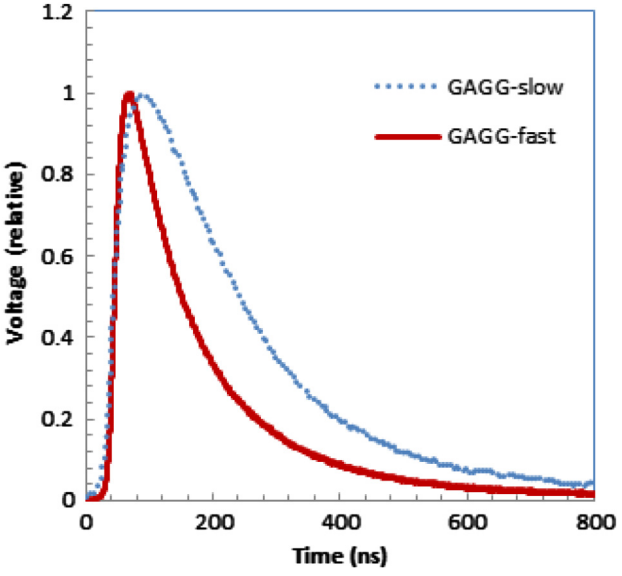

Fig. 3. Pulse shapes of GAGG-F (fast) and GAGG-S (slow) measured by digital oscilloscope.

3.2. Phoswich DOI block detector

(1) Large pixel block

Fig. 5 shows a 2-dimensional histogram and the profiles of the Si-PM-based GAGG DOI large pixel block detector for 662-keV

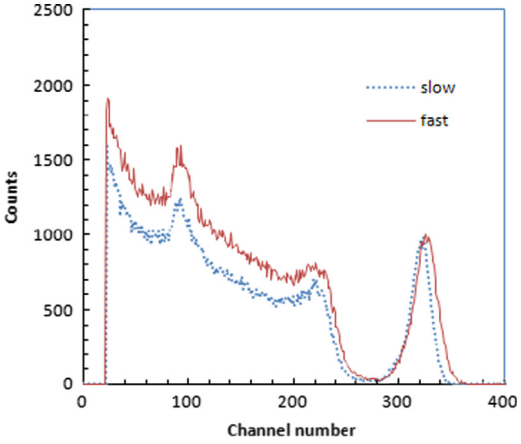

Fig. 4. Energy spectra of GAGG-F (fast) and GAGG-S (slow).

Table 1
Major property and summary of performance of GAGG-F and GAGG-S.

	GAGG-F	GAGG-S
Effective atomic number	53.4	53.9
Density (g/cm^3)	6.63	6.46
Emission light wave length (nm)	520	520
Decay time (ns)	110 ± 2	183 ± 5
Energy resolution (% FWHM)	7.5 ± 0.2	6.3 ± 0.3
Timing resolution (ps)	419 ± 12	1259 ± 50

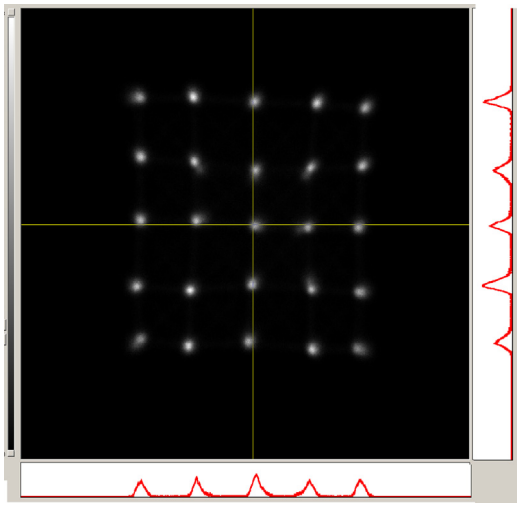

Fig. 5. Two-dimensional histogram of Si-PM-based GAGG DOI large pixel block detector for 662-keV gamma photons.

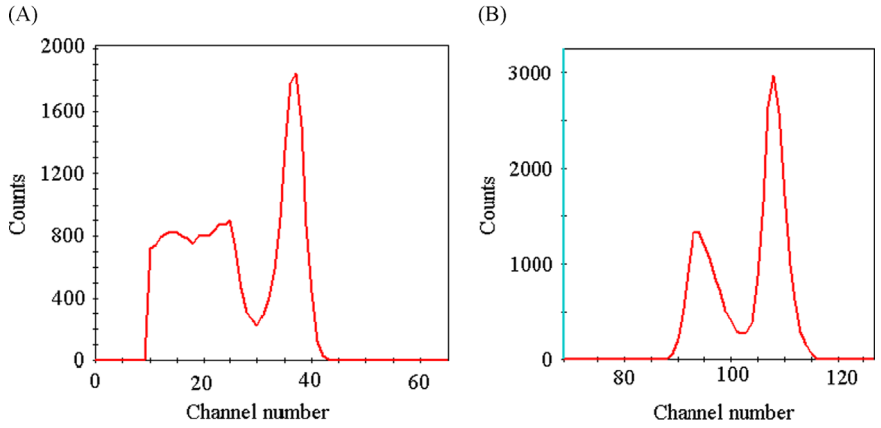

Fig. 6. Energy spectrum (A) and pulse shape spectrum (B) of Si-PM-based GAGG DOI large pixel block detector for 662-keV gamma photons.

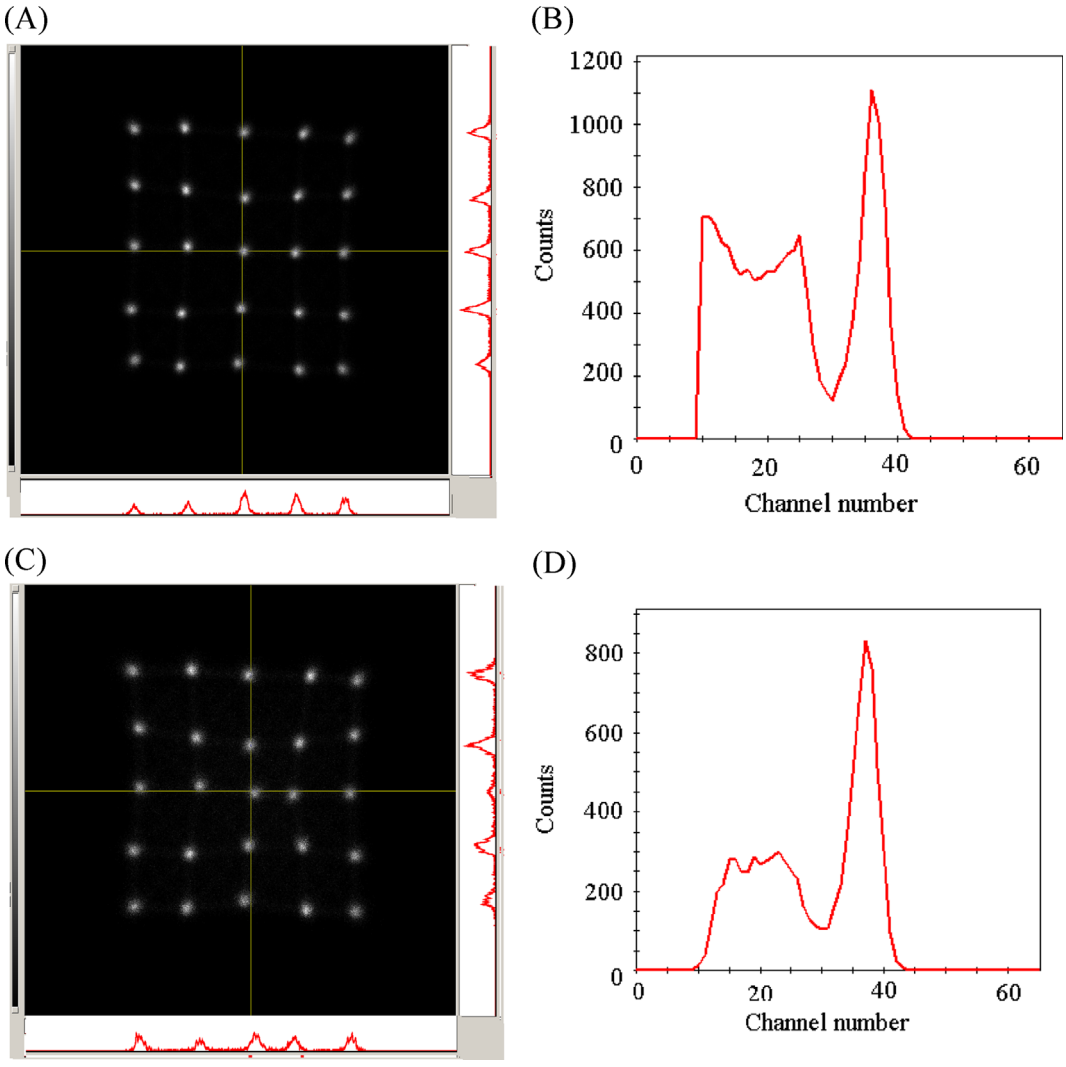

Fig. 7. Two-dimensional histograms (A) and energy spectrum (B) discriminated for GAGG-F, and two-dimensional histograms (C) and energy spectrum (D) discriminated for GAGG-S.

gamma photons. The lower energy threshold was set to 170-keV. The histogram display excellent separation. This amount of histogram separation indicates adequate margins to resolve much smaller scintillators.

Fig. 6(A) shows the energy spectrum of one of the pixels of the Si-PM-based GAGG DOI large pixel block detector for the 662-keV gamma photons. The energy resolution was 14.1% FWHM. Fig. 6(B) shows the pulse shape spectrum of the Si-PM-based GAGG DOI block detector for the 662-keV gamma photons. The right peak corresponds to the upper layer (GAGG-F), and the left corresponds to the bottom layer (GAGG-S). The pulse shape spectrum showed good separation with a peak-to-valley ratio of 8.7.

Fig. 7(A) shows a 2-dimensional histogram discriminated for the right peak (GAGG-F: fast decay) of the pulse shape spectra. The histogram showed better separation than the one in Fig. 5. Fig. 7(B) is an energy spectrum discriminated for the right peak

(GAGG-F: fast decay) of the pulse shape spectra. The energy spectrum showed improved resolution of 13.2% FWHM compared with that without discrimination. Fig. 7(C) shows a 2-dimensional histogram discriminated for the left peak (GAGG-S: slow decay) of the pulse shape spectra. It depicts slightly larger distortion than that discriminated with GAGG-F. Finally, Fig. 7(D) shows an energy spectrum discriminated for the left peak (GAGG-S: slow decay) of the pulse shape spectra. The energy resolution was 14.5% FWHM. It can be seen that the scatter component in the energy spectrum is smaller than that of GAGG-F.

(2) Small pixel block

The 2-dimensional histogram and the profiles of a Si-PM-based GAGG DOI small pixel block detector with the lower energy threshold of 400-keV are illustrated in Fig. 8. The histogram indicated reasonable separation with the peak-to-valley ratios for the horizontal and vertical directions of the profiles were computed to be 1.89 and 1.88, respectively.

Fig. 9(A) shows the energy spectrum of one of its pixels and the energy resolution was 27.5% FWHM. Fig. 9(B) shows a pulse shape spectrum of the Si-PM-based GAGG DOI small pixel block detector. The pulse shape spectrum showed good separation with a peak-to-valley ratio of 6.5.

A 2-dimensional histogram discriminated for the right peak of the pulse shape spectra is illustrated in Fig. 10(A). The histogram showed improved separation than the one in Fig. 8 with the peak-to-valley ratios for the horizontal and vertical directions of the profiles were 2.72 and 2.66, respectively. Fig. 10(B) shows energy spectrum discriminated for the right peak of the pulse shape spectra. An energy resolution of 28.1% FWHM was measured.

Fig. 10(C) shows a 2-dimensional histogram discriminated for the left peak of the pulse shape spectra, exhibiting a different distortion pattern from that discriminated with GAGG-F. The peak-to-valley ratios for the horizontal and vertical directions of the profiles were 1.70 and 1.66, respectively. Fig. 10(D) is an energy spectrum discriminated for the left peak of the pulse shape spectra with the energy resolution was 28.9% FWHM. The scatter component in the energy spectrum is also smaller than that of GAGG-F.

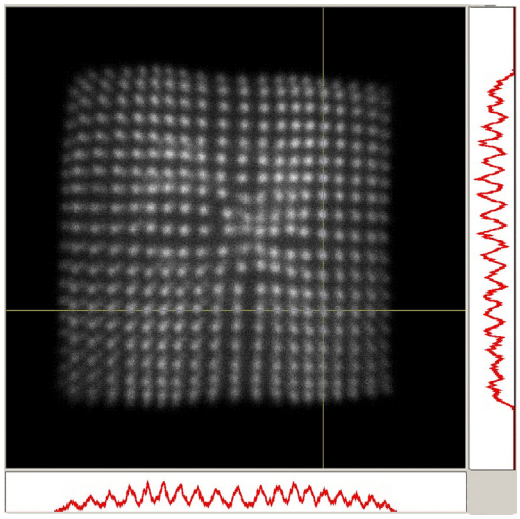

Fig. 8. Two-dimensional histogram of Si-PM-based GAGG DOI small pixel block detector for 662-keV gamma photons.

4. Discussion

We have successfully developed two-layered phoswich DOI block detectors using GAGG-F and GAGG-S. Their decay time difference (73 ns) was sufficient to distinguish these two types of GAGGs by pulse shape analysis. Compared with Si-PM based LGSO phoswich block detector with different Ce concentrations [17], pulse shape spectra of the developed GAGG phoswich block detectors had much better separations, probably because the larger decay time difference for GAGG block detectors. Compared with position sensitive photomultiplier based GSO phoswich block detector with different Ce concentrations [21], pulse shape spectra for both types of detectors showed good separations.

Phoswich DOI block detectors using same types of scintillators are advantageous over those made of different ones. First, as the light outputs of GAGG-F and GAGG-S are similar, a phoswich DOI detector with these GAGGs only requires a single energy window for both DOI layers, simplifying the processing circuits for the phoswich detectors. Another advantage is that since the light transmission properties between GAGG-F and GAGG-S are identical, scintillation light absorption or light transmission reduction as photons propagate through both scintillator types are negligible. Finally, such block detectors may also benefit by having similar densities between the two types of scintillators.

The 2-dimensional distribution of small pixel block detector without pulse shape discrimination (Fig. 8) displayed more blurring than those with discriminations (Fig. 10(A) and (C)). The reason of the blurring without pulse shape discrimination can be explained as follows; the flood maps in Fig. 10(A) and (C) correspond to different crystal array layers in the block detector while 2-dimensional distribution without discrimination is the sum of these two distributions with different shapes. Thus the 2-dimensional distribution without discrimination is more blurred than those with discrimination.

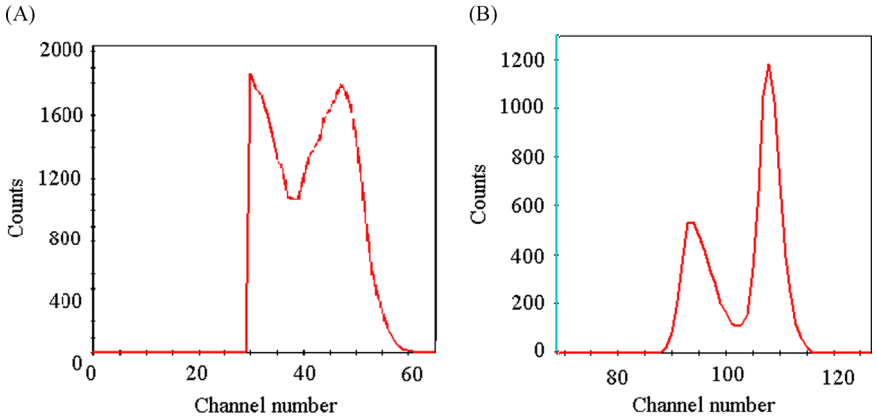

Fig.9. Energy spectrum (A) and pulse shape spectrum (B) of Si-PM-based GAGG DOI small pixel block detector for 662-keV gamma photons.

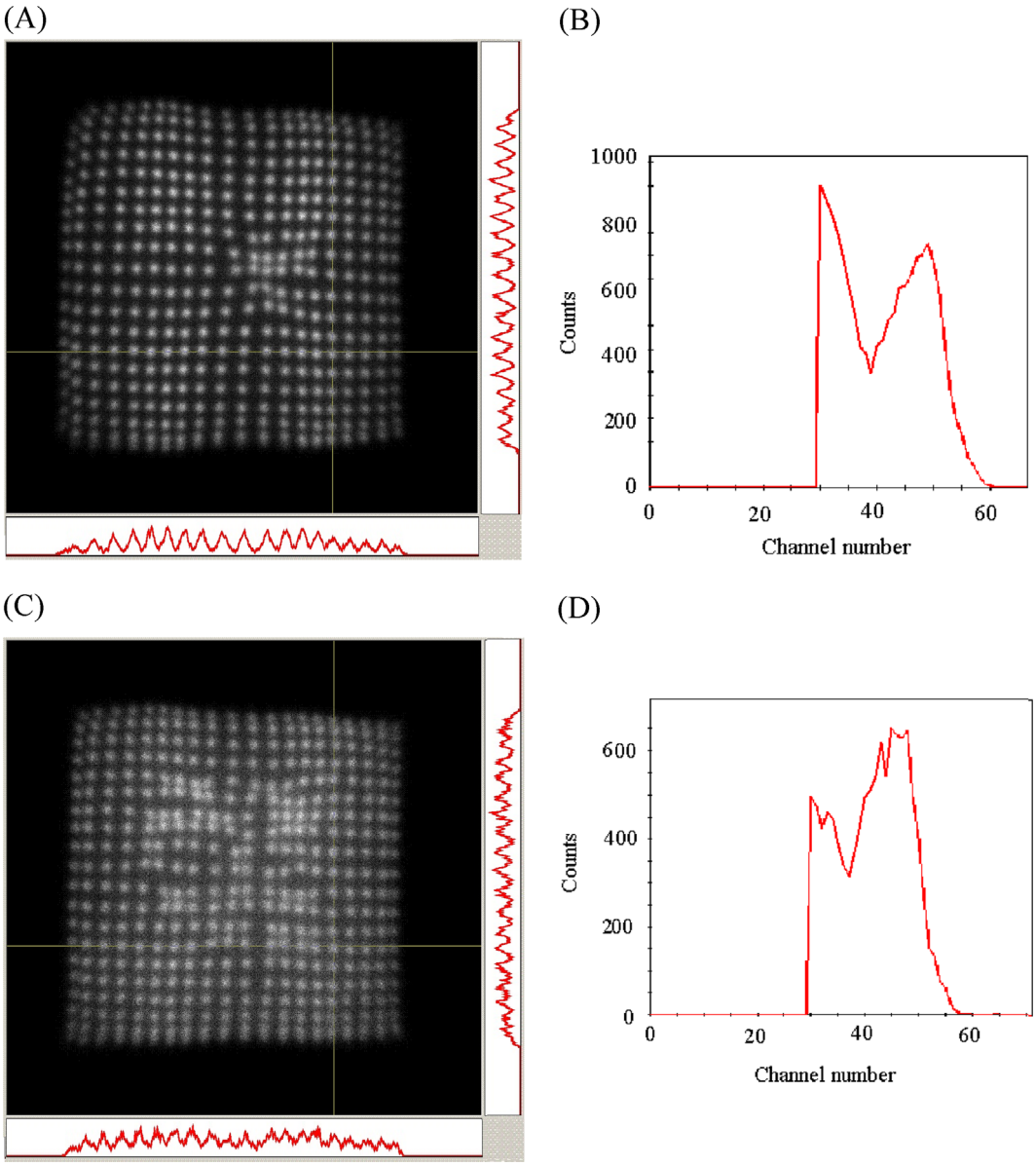

Fig. 10. Two-dimensional histograms (A) and energy spectrum (B) discriminated for GAGG-F, and two dimensional histograms (C) and energy spectrum (D) discriminated for GAGG-S for small pixel block detectors.

Fig. 10(A) (GAGG-F) showed better separation in the 2-dimensional distribution than Fig. 10(C) (GAGG-S). This is probably because the GAGG-F block was located on the upper portion of the block detector (Fig. 2) and contained fewer scattered events in the scintillators that impoved the position accuracy.

The energy spectra of the upper layer (Figs. 7(B) and 10(B)) exhibited higher scatter components than those of the lower layer (Figs. 7(D) and 10(D)). This is due to fact that scattered gamma photons from the Cs-137 gamma source prior to entering the GAGG block, including back scatter in the surrounding materials, have a higher probability of interacting in the upper layer (GAGG-F) than in the lower layer (GAGG-S) because the lower energy scattered photons have shorter attenuation length. Such phenomenon in DOI block detectors based on analog decoding has also been observed and reported by another research group [25].

5. Conclusion

We have developed two types of GAGG phoswich DOI Si-PM block detectors with different crystal dimensions, and the pulse shape spectra as well as the 2-dimensional distributions revealed excellent performance. As GAGG-F and GAGG-S exhibit relatively large decay time difference of 67 ns, accurate pulse shape discrimination is possible. These results indicate that phoswich DOI detectors with two types of GAGGs are promising for developing high resolution PET systems.

Acknowledgements

This work has been supported in part JSPS KAKENHI Grant Number 25253077 of Japan and Quality of Working life (QWL) Program funded by the Ministry of Trade, Industry & Energy of South Korea.

References

[1] K. Kamada, T. Yanagida, T. Endo, K. Tsutumi, Y. Usuki, M. Nikl, Y. Fujimoto, A. Fukabori, A. Yoshikawa, J. Cryst. Growth (2012) 35288.
[2] J.Y. Yeom, S. Yamamoto, S.E. Derenzo, V.C.h. Spanoudaki, K. Kamada, T. Endo, C.S. Levin, IEEE Trans. Nucl. Sci. NS 60 (2) (2013) 988.

[3] S. Yamamoto, J.Y. Yeom, K. Kamada, T. Endo, C.S. Levin, IEEE Trans. Nucl. Sci. NS 60 (2013) 4582.
[4] W.W. Moses, Nucl. Instrum. Methods Phys. Res., Sect. A 648 (Suppl. 1) (2011) S236 (Aug 21).
[5] T. Yamaya, E. Yoshida, T. Inaniwa, S. Sato, Y. Nakajima, H. Wakizaka, et al., Phys. Med. Biol. 56 (4) (2011) 1123.
[6] Y. Shao, X. Sun, K. Lou, X.R. Zhu, D. Mirkovic, F. Poenisch, D. Grosshans, P.E.T. In-beam, Phys. Med. Biol. 59 (13) (2014) 3373.
[7] C.C. Wagner, O. Langer, Adv. Drug Delivery Rev. 63 (7) (2011) 539.
[8] S. Yamamoto, H. Horii, M. Hurutani, K. Matsumoto, M. Senda, 19, 2, 109, 2005.
[9] M. Nikl, A. Yoshikawa, K. Kamada, K. Nejezchleb, C.R. Stanek, J.A. Mareš, K. Blažek, Prog. Cryst. Growth Charact. Mater. 59 (2) (2013) 47 (June).
[10] S. Yamamoto, H. Ishibashi., A. GSO, IEEE Trans. Nucl. Sci. NS 45 (3) (1998) 1069.
[11] R.S. Miyaoka, T.K. Lewellen, H. Yu, D.L. McDaniel, IEEE Trans. Nucl. Sci. NS 45 (3) (1998) 1078.
[12] Y. Yang, Y. Wu, S.R. Cherry, IEEE Trans. Nucl. Sci. NS 56 (5) (2009) 2594.
[13] S.S. James, Y. Yang, Y. Wu, R. Farrell, P. Dokhale, K.S. Shah, S.R. Cherry, Phys. Med. Biol. 54 (14) (2009) 4605.
[14] D.R. Schaart, H.T. van Dam, S. Seifert, R. Vinke, P. Dendooven, H. Löhner, F.J. Beekman., Phys. Med. Biol. 54 (11) (2009) 3501.
[15] T. Tsuda, H. Murayama, K. Kitamura, T. Yamaya, E. Yoshida, T. Omura, H. Kawai, et al., IEEE Trans. Nucl. Sci. NS 51 (5) (2004) 2543.
[16] S. Yamamoto, S. Takamatsu, H. Murayama, K. Minato, IEEE Trans. Nucl. Sci. NS 51 (1) (2005).
[17] S. Yamamoto, M. Imaizumi, T. Watabe, H. Watabe, Y. Kanai, E. Shimosegawa, J. Hatazawa, Phys. Med. Biol. 55 (19) (2010) 5817.
[18] S. Yamamoto, M. Imaizumi, Y. Kanai, M. Tatsumi, M. Aoki, E. Sugiyama, M. Kawakami, et al., Ann. Nucl. Med. 24 (2) (2010) 89.
[19] S. Yamamoto, H. Watabe, Y. Kanai, T. Watabe, M. Aoki, E. Sugiyama, K. Kato, J. Hatazawa, Med. Phys. 39 (11) (2012) 6660.
[20] S. Yamamoto, M. Honda, T. Oohashi, K. Shimizu, M. Senda, IEEE Trans. Nucl. Sci NS 56 (5) (2011).
[21] T. Yamaya, E. Yoshida, C. Toramatsu, M. Nishimura, Y. Shimada, N. Inadama, et al., Ann. Nucl. Med. 23 (2) (2009) 183.
[22] F. Sanchez, L. Moliner, C. Correcher, A. Gonzalez, A. Orero, M. Carles, et al., Med. Phys. 39 (2) (2012) 643.
[23] K. Kamada, P. Prusa, M. Nikl, V. Kochurikhin, T. Endo, K. Tsutumi, H. Sato, et al., Opt. Mater. 36 (12) (2014) 1942.
[24] J.Y. Yeom, R. Vinke, C.S. Levin, Phys. Med. Biol. 58 (4) (2013) 1207.
[25] E. Yoshida, K. Kitamura, K. Shibuya, F. Nishikido, T. Hasegawa, T. Yamaya, et al., IEEE Trans. Nucl. Sci. NS 55 (5) (2008) 2475.